

## hPuf-A/KIAA0020 Modulates PARP-1 Cleavage upon Genotoxic Stress

Hao-Yen Chang<sup>1</sup>, Chi-Chen Fan<sup>2</sup>, Po-Chen Chu<sup>1</sup>, Bo-En Hong<sup>1</sup>, Hyeon Jeong Lee<sup>3</sup>, and Mau-Sun Chang<sup>1,4</sup>

### Abstract

Human hPuf-A/KIAA0020 was first identified as a new minor histocompatibility antigen in 2001. Its zebrafish orthologue contains six Pumilio-homology RNA-binding domains and has been shown to participate in the development of eyes and primordial germ cells, but the cellular function of hPuf-A remains unclear. In this report, we showed that hPuf-A predominantly localized in the nucleoli with minor punctate signals in the nucleoplasm. The nucleolar localization of hPuf-A would redistribute to the nucleoplasm after the treatment of RNA polymerase inhibitors (actinomycin D and 5,6-dichlorobenzimidazole riboside) and topoisomerase inhibitors [camptothecin (CPT) and etoposide]. Interestingly, knockdown of hPuf-A sensitized cells to CPT and UV treatment and cells constitutively overexpressing hPuf-A became more resistant to genotoxic exposure. Affinity gel pull-down coupled with mass spectrometric analysis identified PARP-1 as one of the hPuf-A interacting proteins. hPuf-A specifically interacts with the catalytic domain of PARP-1 and inhibits poly(ADP-ribose)ylation of PARP-1 *in vitro*. Depletion of hPuf-A increased the cleaved PARP-1 and overexpression of hPuf-A lessened PARP-1 cleavage when cells were exposed to CPT and UV light. Collectively, hPuf-A may regulate cellular response to genotoxic stress by inhibiting PARP-1 activity and thus preventing PARP-1 degradation by caspase-3. *Cancer Res*; 71(3); 1126–34. ©2011 AACR.

### Introduction

PUF family proteins are named for the initially identified members *Drosophila melanogaster* Pumilio and *Caenorhabditis elegans* fem-3 binding factor (1–3). The main structural feature of PUF proteins is the presence of 8 Pumilio homology domains or PUF domains, each consisting of 35 to 39 amino acids capable of associating with the 3'-untranslated region (3'-UTR) of target mRNAs to promote mRNA degradation and translational repression (1–3). Recently, a new member of zebrafish PUF family proteins, Puf-A, was identified to participate in the eye and primordial germ-cell development (4). zfPuf-A contains a unique 6 PUF-repeat domain, similar to but distinct from the feature of 8 PUF repeats in other PUF members. Knockdown of Puf-A in zebrafish embryos resulted in a small head phenotype and abnormal primordial germ-cell

migration. The expression of Puf-A is unique in the most primitive follicles in adult ovaries but declines at later stages of folliculogenesis. In addition, the target mRNAs of zfPuf-A, *Prdm1a*, *spata2*, *tex10*, *rbb4*, *ddx3*, and *zp2.2* mRNAs, isolated by RNA-immunoprecipitation have a variety of functions in the zebrafish embryo development (4). Nevertheless, how zfPuf-A regulates the translation of its associated mRNA is still unclear.

In response to DNA strand breaks, poly(ADP-ribose)ylation is a crucial posttranslational modification for DNA repair or cell death. PARP-1 senses DNA nicks and uses NAD<sup>+</sup> to transfer ADP-ribose moieties to nuclear acceptor or to PARP-1 itself. The poly(ADP-ribose), or pADPr, is further extended to a linear or branched polymer with variable lengths. DNA repair proteins and other factors are then recruited either to promote DNA repair or to induce cell death (5, 6). It has been shown that PARP-1 mainly localizes in the nucleoplasm but approximately 40% of PARP-1 can be found in the nucleoli. Delocalization of nucleolar PARP-1 to the nucleoplasm was reported when cells were exposed to genotoxic insults such as camptothecin (CPT) and UV light (7). The pADPr polymer has been reported as a death signal (8), and PARP-1 activation is required for the translocation of mitochondrial apoptosis-inducing factor (AIF) into the nucleus to mediate programmed cell death (9, 10). During apoptosis, PARP-1 is cleaved by caspases, recognizing the DEVD motif within DNA-binding domain of PARP-1 and leaving 24- and 89-kDa fragments to inactivate the enzymatic activity of poly(ADP-ribose)ylation (11). The N-terminal

**Authors' Affiliations:** <sup>1</sup>Institute of Biochemical Sciences, College of Life Science, National Taiwan University; <sup>2</sup>Department of Physiology, Mackay Memorial Hospital; <sup>3</sup>Department of Biochemical Science and Technology, College of Life Science, National Taiwan University; and <sup>4</sup>Institute of Biological Chemistry, Academia Sinica, Taipei, Taiwan

**Note:** Supplementary data for this article are available at Cancer Research Online (<http://cancerres.aacrjournals.org/>).

**Corresponding Author:** Mau-Sun Chang, Institute of Biochemical Sciences, National Taiwan University No. 1, Sec. 4, Roosevelt Road, Taipei 10617, Taiwan. Phone: 886-2-3366-9837; Fax: 886-2-2363-5038; E-mail: mschang@ntu.edu.tw

doi: 10.1158/0008-5472.CAN-10-1831

©2011 American Association for Cancer Research.

24-kDa fragment binds DNA breaks irreversibly to inhibit DNA repair and pADPr formation and then stimulate apoptosis (12, 13). The C-terminal 89-kDa fragment interacts with intact PARP-1 to block the PARP homodimerization, which is essential for poly(ADP-ribosylation) activity (14).

In 2001, an HLA-A\*0201-restricted minor histocompatibility antigen (mHAg), HA-8, is identified as a new mHAg. The HA-8 peptide RTLDKVLEV is derived from amino acid residues 289 to 297 in *KIAA0020*, a gene of unknown function located on chromosome 9 (15). Amino acid alignment showed that KIAA0020 shares 63% of identity with zPuf-A, indicating that hPuf-A/KIAA0020 is a human orthologue of zebrafish Puf-A. In this study, we determined the subcellular localization of hPuf-A and analyzed cellular responses to genotoxic treatments under conditions that the expression of hPuf-A is manipulated. These results provide novel findings that the presence of Puf-A prevents PARP-1 from caspase degradation and thus regulates cell viability to genotoxic stress.

## Materials and Methods

### Antibodies

Mouse anti-hPuf-A monoclonal antibody (mAb) was raised against 6xHis-tagged hPuf-A recombinant protein. Mouse anti-PARP-1 and anti-HA antibodies were purchased from Santa Cruz Biotech. Mouse anti-RPA1, anti-RPA2, and anti- $\gamma$ -H2AX were from Cell Signaling. Mouse anti-XRCC1 was from Thermo Scientific. Mouse anti- $\beta$ -actin antibody was from Novus Biologicals.

### Small interfering RNA

The siRNA duplexes sihPuf-A#1, 5'-GGACAAAGUGUUA-GAGGUAdTdT-3' and sihPuf-A#2, 5'-CGGAAGAGCUUAUG-GGAAdTdT-3' were synthesized from Thermo Scientific Dharmacon and used to knockdown the expression of hPuf-A.

### Isolation of nucleoplasmic protein

Cells were lysed and fractionated as described (16). Briefly,  $2 \times 10^6$  cells were washed with PBS and resuspended in 200  $\mu$ L of buffer A (10 mmol/L HEPES at pH 7.9, containing 10 mmol/L KCl, 1.5 mmol/L MgCl<sub>2</sub>, 0.34 mol/L sucrose, 10% glycerol, 1 mmol/L dithiothreitol, and protease inhibitors). Triton X-100 (0.1%) was added and followed by 5 minutes of incubation on ice. Nuclei were collected by centrifugation at low speed (1,300  $\times g$ , 5 min, 4°C). The supernatant was clarified by high-speed centrifugation (20,000  $\times g$ , 15 minutes, 4°C) to obtain the cytoplasmic soluble fraction. Nuclei were then washed once with buffer A, resuspended in 200  $\mu$ L of buffer B (10 mmol/L HEPES at pH 7.9, containing 3 mmol/L EDTA, 0.2 mmol/L EGTA, 1 mmol/L DTT, and protease inhibitors), and incubated on ice for 30 minutes. Soluble nuclear fraction was collected by centrifugation (1,700  $\times g$ , 5 minutes, 4°C) and determined by Western blot analysis.

### Genotoxic treatment

Unless otherwise stated, cells were either exposed to UV (30 J/m<sup>2</sup>) and CPT (10  $\mu$ mol/L) for 2 hours or UV (20 J/m<sup>2</sup>) and CPT (5  $\mu$ mol/L) for 24 hours.

### Detection of apoptotic cells

Apoptotic cells were labeled with FITC-conjugated Annexin V (Sigma-Aldrich) for 15 minutes in the dark and analyzed by FACSCalibur (Becton Dickinson).

### MTT assay

Cells were seeded in a 24-well tissue culture plate and treated with CPT at the indicated concentrations. After 24 hours, MTT (Sigma-Aldrich) solution (0.5 mg/mL) was added to each well. After incubation for 2 hours at 37°C, formazan crystals in viable cells were solubilized in 200  $\mu$ L of DMSO. The soluble formazan product was quantified using an ELISA reader at 570 nm.

### Mass spectrometry for the identification of hPuf-A interacting proteins

HEK293 cells were transfected with plasmids expressing HA-tagged hPuf-A for 48 hours and cell lysates were harvested in the lysis buffer (50 mmol/L Tris, pH 8, 150 mmol/L NaCl, 1% NP-40, 1% Triton X-100, and protease inhibitors). Preclearing of lysates was done by the incubation of protein A agarose and subsequent immunoprecipitation was conducted by anti-HA-agarose (Sigma-Aldrich). After extensive washing, HA-hPuf-A-associated complex was released by boiling in SDS sample buffer and subjected to SDS-PAGE. The Coomassie blue-stained gel was sliced into 2-mm wide pieces for in-gel digestion, and the trypsin-digested peptide fragments were analyzed with liquid chromatography/tandem mass spectrometry (LC/MS-MS; service provided by Academia Sinica, Taipei, Taiwan). LC was conducted on an Agilent 1100 series HPLC system (Agilent Technologies), with a micro-T for flow splitting coupled to an LTQ-Orbitrap XL hybrid mass spectrometer (Thermo Electron) equipped with a PicoView nanospray interface (New Objective).

### In vitro poly(ADP-ribosylation)

HA-tagged PARP-1 was transfected into 293T cells and pulled down with anti-HA agarose beads (Sigma-Aldrich). Samples were incubated in PAR reaction buffer (50 mmol/L Tris-HCl, pH 8.0, 4 mmol/L MgCl<sub>2</sub>, 0.25 mmol/L DTT, 1 $\times$  protease inhibitors) in the presence of 5 pmol annealed double-stranded oligomer (5'-GATGGAATTCC-3') and supplemented with <sup>32</sup>P-NAD (10  $\mu$ Ci) at 30°C for 3 minutes. Reactions were stopped by the addition of SDS-PAGE loading buffer and boiling for 5 minutes at 95°C. Samples were subjected to SDS-PAGE and the dried gel was exposed to X-ray film at room temperature.

### Cell manipulation

Lentiviral production, immunofluorescence, immunoprecipitation, siRNA transfection, and isolation of chromatin-associated proteins were carried out as previously reported (17) and are described in Supplementary Data.

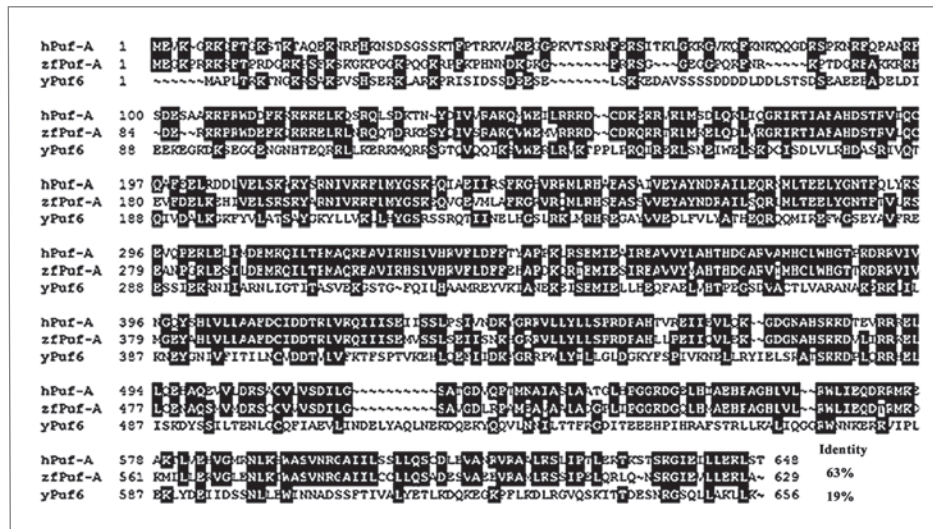


Figure 1. Amino acid alignment of human hPuf-A/KIAA0020 with zfpPuf-A (zgc66377) and scPuf6p (AAB64938). Identical amino acid residues are highlighted with closed boxes. Dashes have been applied for maximum alignment.

## Results

### Human hPuf-A/KIAA0020 is an orthologue of zebrafish Puf-A and yeast Puf6p

Amino acid alignment showed that hPuf-A/KIAA0020 shares 63% sequence identity with zebrafish Puf-A and contains 6 distinct PUF domains (a.a. 165–200, 201–236, 237–273, 350–385, 386–422, and 424–460) that are highly conserved in zebrafish Puf-A. Database search also reveals that Puf-A is potentially a homologue of yeast Puf6p with 19% sequence identity (Fig. 1). In *Saccharomyces cerevisiae*, Ash1p is a protein determinant for mating-type switch by establishing asymmetry of *HO* endonuclease expression. yPuf6p represses *ASH1* mRNA translation, and this repression is relieved by phosphorylation of the N-terminal region of yPuf6p mediated by casein kinase 2. Inhibition of phosphorylation at Ser31, Ser34, and Ser35 of yPuf6p increases its translational repression and results in *ASH1* mRNA delocalization. In addition, yPuf6p has been shown to localize in the nucleus (18–20). Nonetheless, human hPuf-A contains a distinct N-terminal region with a low homology with zfpPuf-A and yPuf6p. Besides, the absence of conserved Ser31, Ser34, and Ser35 residues in hPuf-A and zfpPuf-A (Fig. 1) indicates that a different regulatory mechanism in different species may prevail among these Puf-A orthologues.

### hPuf-A is a nucleolar protein

The specificity of anti-hPuf-A mAb was determined by Western blot analysis (Fig. 2A). Because yPuf6p is a nuclear protein, we speculated that hPuf-A might also be localized in the nucleus. Unexpectedly, immunofluorescence staining showed that hPuf-A predominantly located in the nucleoli with some punctate patterns in the nucleoplasm. Transient expression of HA-tagged hPuf-A also appeared in the nucleoli (Fig. 2B), indicating that the subcellular localization of hPuf-A is different from that of yPuf6p. This result is supported by a recent report in which KIAA0020 has been

identified as a nucleolar protein by nucleolar proteome analysis (21).

### Identification of nucleolar localization signal in hPuf-A

To determine the nucleolar localization region of hPuf-A responsible for its targeting to the nucleolus, a variety of deletion mutants of hPuf-A were in-frame fused with the C-terminus of the enhanced green fluorescent protein (GFP; Fig. 3). The full-length GFP-tagged hPuf-A (GFP-hPuf-A<sub>FL</sub>) was unequivocally distributed to the nucleoli. GFP-hPuf-A<sub>1–105</sub> localized in the cytoplasm. In contrast, GFP-hPuf-A<sub>1–118</sub>, which contains a putative nucleolar localization signal (NoLS, KKPKWDDFKKKKK), largely located in the nucleoli. GFP-hPuf-A<sub>119–648</sub>, a construct without the N-terminus and NoLS of hPuf-A, mainly distributed in the cytoplasm. Other deletion mutagenesis aiming to deprive of certain PUF domains, but

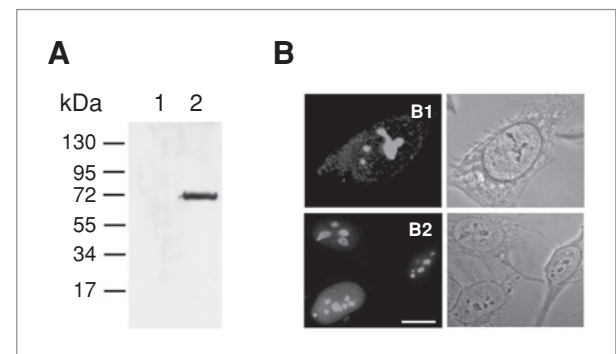
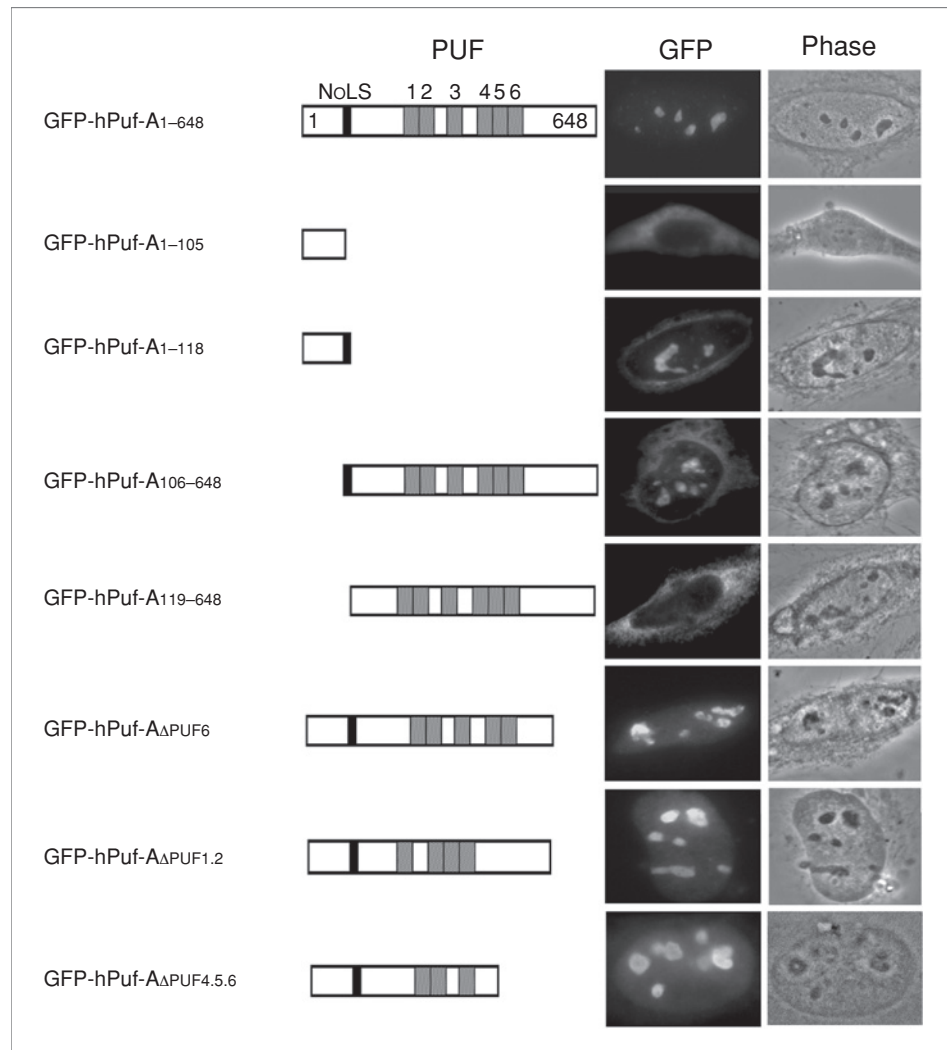


Figure 2. hPuf-A localized in the nucleolus. A, whole-cell extracts prepared from HeLa cells were analyzed by Western blotting, using anti-hPuf-A mAb preincubated with 6xHis-tagged hPuf-A recombinant protein (lane 1) and anti-hPuf-A mAb with no treatment (lane 2). B, endogenous (B1) and HA-hPuf-A-transfected (B2) HeLa cells were fixed in cold methanol (–20°C) and immunostained with anti-hPuf-A and HA mAbs, respectively. Phase-contrast micrographs show the same field as the fluorescently labeled cell. Bar, 10 μm.





**Figure 3.** Identification of a nucleolar localization signal in hPuf-A. Deletion constructs of hPuf-A were fused to the C-terminus of GFP protein and transfected into HeLa cells. Green fluorescence images were recorded by Leica immunofluorescence microscope D6000. Nucleoli are shown by phase-contrast images.

leaving the NoLS intact, did not alter the nucleolar localization of hPuf-A (Fig. 3), indicating that the nucleolar localization signal resides in amino acid residue 106 to 118 of hPuf-A.

#### Delocalization of hPuf-A to the nucleoplasm with genotoxic agents

Because hPuf-A is a member of PUF family proteins, we checked whether an interference of RNA transcription could affect the localization of hPuf-A. As anticipated, the addition of actinomycin D, an inhibitor of RNA polymerase I, resulted in 90% of cells displaying nucleoplasm rather than nucleolar distribution of hPuf-A. A modest decrease in distribution of hPuf-A to the nucleoplasm (approximately 60% of cells) was observed in cells treated with 5,6-dichlorobenzimidazole riboside (DRB), an inhibitor of RNA polymerase II and casein kinase 2). It has been suggested that many nucleolar proteins are responsive to genotoxic treatments and oxidative stress. We tested whether hPuf-A nucleolar trafficking was affected by genotoxic agents. HeLa cells were exposed to a variety of

genotoxic agents (Supplementary Table S1). Interesting, approximately 60% of HeLa cells treated with topoisomerase inhibitors (CPT, topotecan hydrochloride, etoposide/VP16, and amsacrine hydrochloride) and 40% of HeLa cells irradiated with UV light showed a redistribution of hPuf-A to the nucleoplasm (Fig. 4A and Supplementary Table S1). Western blot analysis did not show a significant change in the amount of hPuf-A protein after the exposure to CPT and UV light (Fig. 4B), indicating that the redistribution of hPuf-A was due to protein relocation but not due to degradation or *de novo* protein synthesis. Although soluble nucleoplasmic hPuf-A was not isolated by a traditional density gradient fractionation (data not shown), possibly due to its RNA-binding capacity, subcellular fractionation showed an elevation of Puf-A in the nucleoplasmic fraction after CPT treatment (Fig. 4C). No delocalization was found in cells 4 hours after treatment with mitomycin C, wortmannin,  $\gamma$ -irradiation, and MG132 (Supplementary Table S1), suggesting that the localization of hPuf-A in the nucleoli is

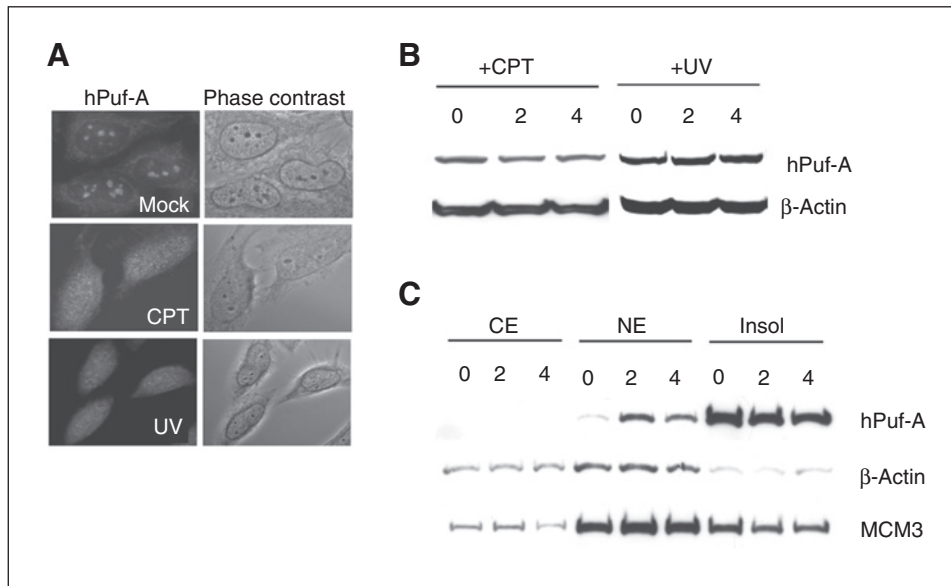


**Figure 4.** Relocalization of hPuf-A postgenotoxic treatment. A, HeLa cells were exposed to CPT and UV light for 2 hours and immunostained with anti-hPuf-A mAb. Nucleoli are shown by phase-contrast images. B, HeLa cells were exposed to CPT (10  $\mu\text{mol/L}$ ) and UV light (30  $\text{J/m}^2$ ) and whole-cell extracts were collected at the indicated times for Western blot analysis. C, cytosolic (CE), nuclear (NE), and insoluble (Insol) extracts of HeLa cells postgenotoxic treatments were prepared for immunoblotting analysis.

highly dependent on the activity of RNA polymerase I/II and, to a less extent, of topoisomerase I/II.

#### Knockdown and overexpression of hPuf-A

We employed 2 hPuf-A siRNA duplexes, sihPuf-A#1 and sihPuf-A#2, to silence hPuf-A expression. Firefly luciferase siRNA duplex was used as a control. The total amount of hPuf-A protein was significantly reduced at 72 hours after siRNA transfection in both HeLa and U2OS cells (Fig. 5A). No significant alteration of cell-cycle progression was found in sihPuf-A-transfected cells. The transcription of 18S and 28S rRNA was not affected by hPuf-A depletion (Supplementary Fig. S1). The depletion of hPuf-A sensitized cells to apoptosis after UV and CPT treatment. Genotoxic exposure significantly lowered the cell viability in hPuf-A-depleted cells compared with that of control siRNA for luciferase (siLuc)-transfected cells (Supplementary Fig. S2A). Mitomycin C, which did not result in the delocalization of hPuf-A from the nucleolus, could not reduce cell viability in hPuf-A-knockdown cells (Supplementary Fig. S2B). An increment in the apoptotic population of hPuf-A-depleted cells with Annexin V staining was found after CPT treatment (Fig. 5B), indicating that the absence of hPuf-A did not impair cell-cycle progression but resulted in apoptosis after genotoxic treatments.

We further examined whether constitutive expression of hPuf-A rendered cells resistant to genotoxic insults. U2OS cells were transduced with control and hPuf-A-expressing lentivirus and 2 independent clones (Lenti-hPuf-A#1 and Lenti-hPuf-A#2), with high hPuf-A expression levels were confirmed by immunoblotting (Fig. 5C). hPuf-A-overexpressing cells had a higher viability than control cells after genotoxic treatments (Supplementary Fig. S2C). hPuf-A<sub>119-648</sub>, a deletion construct without the N-terminus and NoLS of hPuf-A, was transiently transfected into U2OS cells and then treated with CPT. The cell viability of hPuf-A<sub>119-648</sub> was similar to that of control HA-

transfected U2OS cells but lower than hPuf-A<sub>FL</sub> (Supplementary Fig. S2D). Annexin V staining showed a reduction in the apoptotic population of hPuf-A-overexpressing cells with CPT treatment (Fig. 5D). In addition, we tested the sensitivity of hPuf-A-knockdown and -overexpressing cells to CPT in colony formation assay. Despite a notable decrease in hPuf-A-depleted cells in cell viability at 2 days post-CPT treatment, the siRNA-transfected cells were not viable to form colonies at 10 days post-CPT exposure, possibly due to a preincubation of transfection reagent. In contrast, hPuf-A-overexpressing cells were significantly resistant to CPT exposure compared with control cells with more surviving colonies (Supplementary Fig. S3), suggesting that CPT-triggered apoptosis was prohibited in cells constitutively expressing hPuf-A.

#### hPuf-A interacted with PARP-1

To identify hPuf-A interacting proteins, human embryonic kidney 293 cells were transfected with HA-tagged hPuf-A and cell extracts were immunoprecipitated with anti-HA antibody and used for MS analysis. Two tryptic peptides corresponding to fragments of human PARP-1 were identified (Supplementary Fig. S4). To test whether hPuf-A interacted with PARP-1 in mammalian cells, endogenous cell extracts were reciprocally immunoprecipitated with anti-hPuf-A and anti-PARP-1 antibodies and immunoblotted with the other antibodies. Western blot analysis revealed that hPuf-A and PARP-1 were in the same immunocomplex (Fig. 6A). Simultaneous labeling of HeLa cells with anti-hPuf-A and anti-PARP-1 antibodies showed overlapping areas of staining in the nucleoli before genotoxic exposure but in the nucleoplasm after CPT and UV treatment (Fig. 6B), indicating that the interaction of hPuf-A and PARP-1 took place in the nucleoli before genotoxic exposure and in the nucleoplasm after genotoxic treatment. Nonetheless, the depletion of hPuf-A did not alter the nucleolar distribution of PARP-1 (Supplementary Fig. S5).

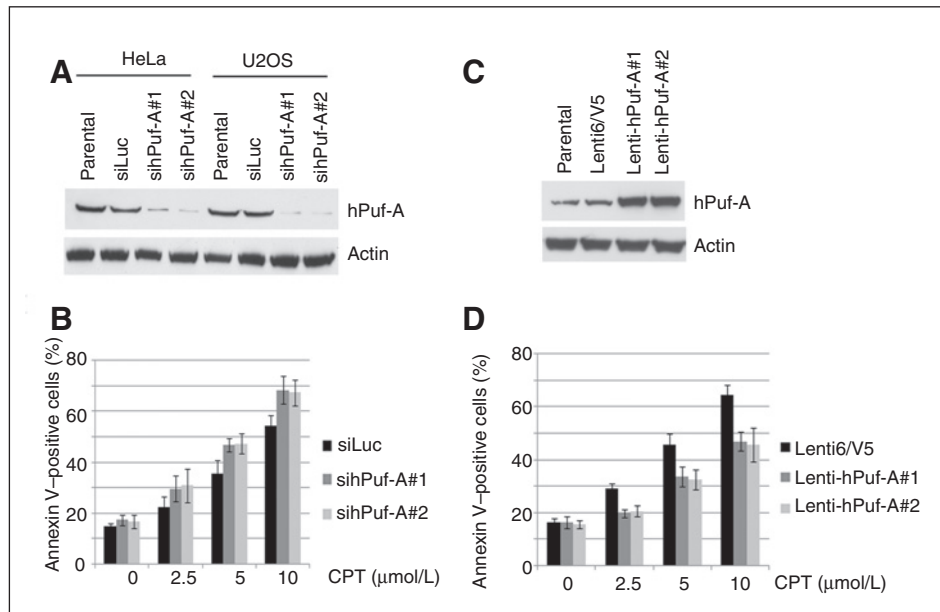


**Figure 5.** hPuf-A affects cell viability in response to genotoxic insults. A, HeLa and U2OS cells were transfected with control luciferase (siLuc) or hPuf-A siRNA duplexes for 72 hours and cell extracts were prepared for Western blot analysis.  $\beta$ -Actin was used as a loading control. B, control and hPuf-A siRNA-transfected U2OS cells were treated with different doses of CPT for 24 hours and apoptotic cells were labeled with FITC-conjugated Annexin V for flow cytometric analysis. The data shown are means  $\pm$  SDs of 3 independent experiments. C, control (Lenti6/V5) and hPuf-A lentivirus were transduced into U2OS cells. Antibiotic resistant clones (Lenti-hPuf-A#1 and Lenti-hPuf-A#2) were selected for immunoblotting analysis with anti-hPuf-A antibody. D, control and hPuf-A stably expressing U2OS cells were exposed to different doses of CPT for 24 hours and apoptotic cells were determined with Annexin V for flow cytometric analysis. The data shown are means  $\pm$  SDs of 3 independent experiments.

Structurally, PARP-1 is composed of 3 regions: DNA-binding domain (DBD) a.a. 1–373; automodification domain (AD) a.a. 374–533; and catalytic domain (CD) a.a. 534–1,014 (22). Immunoprecipitation experiments showed that hPuf-A pulled down HA-tagged catalytic domain, but not DBD or AD, of PARP-1 (Fig. 6C). *In vitro* poly(ADP-ribosylation) revealed that pADPr activity of PARP-1 was remarkably inhibited by hPuf-A (Fig. 6D).

#### hPuf-A attenuated PARP-1 cleavage by caspase-3

The degradation product p89 of PARP-1 by caspase-3 was increased in hPuf-A-depleted cells but decreased in hPuf-A-overexpressing cells post-UV or CPT treatment. Interestingly, the cleaved caspase-3 was also affected in hPuf-A-depleted and -overexpressing cells (Fig. 7A). The enhanced PARP-1 cleavage in hPuf-A knockdown cells exposed to CPT was blocked by Z-DEVD-FMK (Fig. 7B), a caspase-3 inhibitor, suggesting that PARP-1 cleavage is prevented by the binding of hPuf-A. PARP-1 could be immunoprecipitated in the presence of Z-DEVD-FMK (Supplementary Fig. S6A). We did not detect a difference in cytochrome *c* in the cytosolic fraction at 4 hours post-CPT treatment (Supplementary Fig. S6B); nonetheless, we found a decreased chromatin-associated fraction of PARP-1 accompanied with elevated amounts of phosphorylated RPA2 (a single-strand binding protein) and  $\gamma$ -H2AX (a marker of double-strand breaks) in hPuf-A-depleted cells (Fig. 7C), indicating that hPuf-A regulates caspase-3 activity distal to the mitochondrial outer membrane permeabilization. Together, these results strongly suggest that the presence of

hPuf-A reduces the poly(ADP-ribosylation) activity of PARP-1 and regulates the degradation of PARP-1 by caspase-3 during apoptosis.

#### Discussion

On the basis of our studies, a novel function of hPuf-A has been identified to attenuate the poly(ADP-ribosylation) activity of PARP-1. hPuf-A predominantly localizes in the nucleoli and its nucleolar location is redistributed after actinomycin D, DRB, and CPT treatments. Deficiency of hPuf-A sensitizes cells to genotoxic stress; conversely, overexpression of hPuf-A renders cells resistant to genotoxic exposure. These observations link hPuf-A to the regulation of PARP-1 degradation by caspase-3.

The nucleus is a highly ordered structure that contains ribosomal DNA repeats within the chromosomes and is recognized to participate in ribosome biogenesis. Nonetheless, it is also suggested that the nucleolus has multiple functions in mitosis regulation, cell-cycle progression, and stress response (23). These functions are highly associated with protein sequestration and release within the nucleolar compartment and are responsive to metabolic fluctuations (24). The retention of nucleolar proteins in the nucleolus depends on their interactions with other nucleolar proteins or RNA molecules (25). In this study, we have determined a nucleolar targeting sequence, KKPkwDDDFKkkkkk, of hPuf-A. Deletion mutants of hPuf-A without this region could not target hPuf-A to the nucleolus. Although the knockdown of hPuf-A did not affect

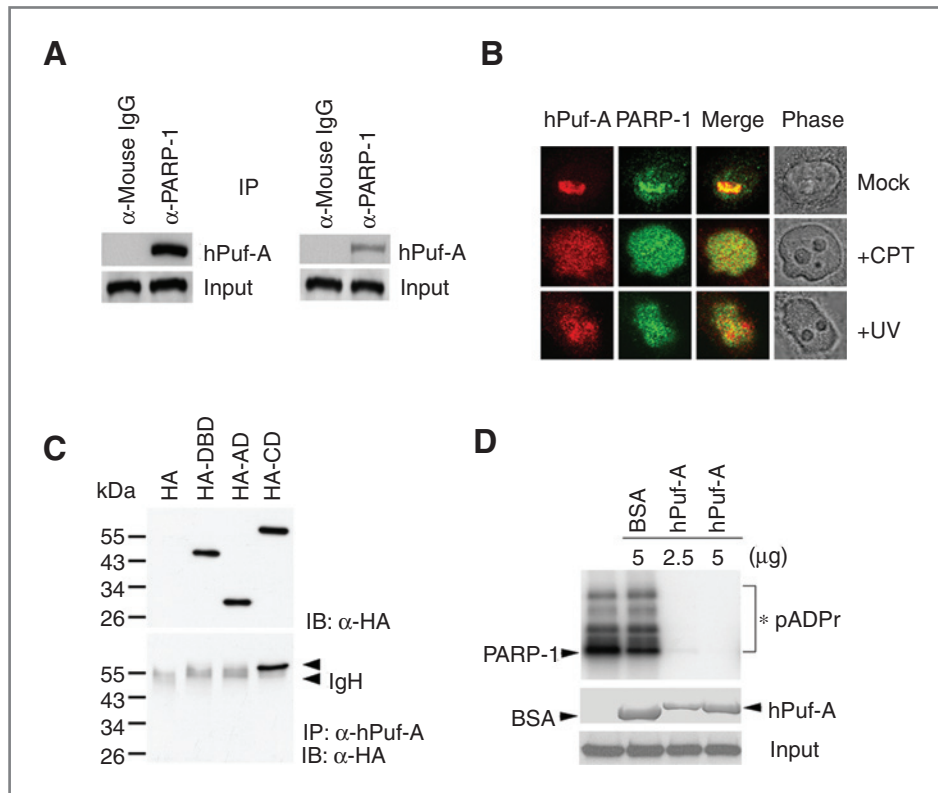


**Figure 6.** PARP-1 is an hPuf-A interacting protein. **A**, endogenous HeLa cell extracts were immunoprecipitated with anti-hPuf-A and anti-PARP-1 antibodies immunoblotted with the opposite antibodies. Input, the same amount of cell extracts for immunoprecipitation blotted by anti-hPuf-A antibody. **B**, HeLa cells were mock-treated or treated with UV and CPT for 2 hours and labeled with a mixture of anti-hPuf-A mAb (red) and anti-PARP-1 polyclonal antibody (green). The images of hPuf-A and PARP-1 are overlaid to show the colocalized areas appearing in yellow. Phase-contrast micrographs show the same field as the fluorescently labeled cell. **C**, HA-tagged DBD, AD, and CD of PARP-1 were transiently transfected into 293T cells. Total cell extracts were immunoprecipitated with anti-hPuf-A antibody and then immunoblotted with anti-HA antibody. **D**, 293T cells were transfected with HA-PARP-1 and pulled down by anti-HA agarose. *In vitro* poly(ADP-ribose)ylation assay was conducted by incubating HA-PARP-1 and  $^{32}\text{P}$ -NAD $^{+}$  supplemented with bovine serum albumin (BSA) or purified 6xHis-hPuf-A.

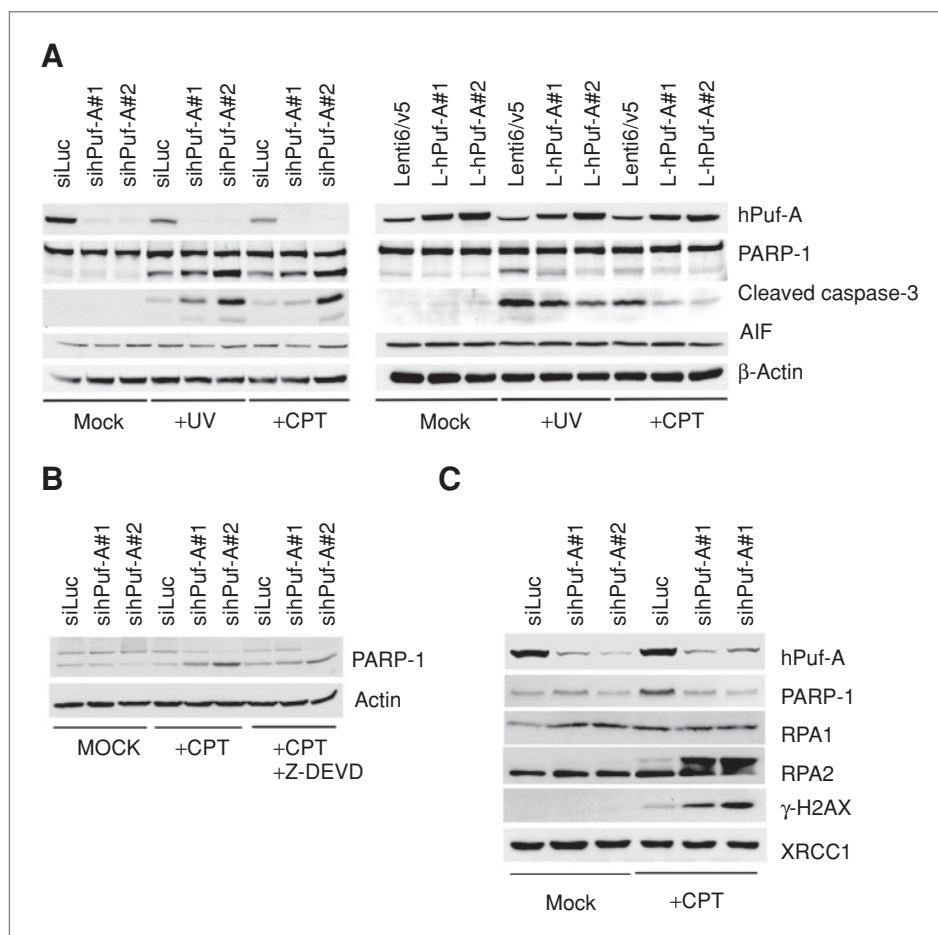
the transcription of 18S and 28S rRNA (Supplementary Fig. S2), the localization of hPuf-A is responsive to RNA transcription inhibitors (Supplementary Table S1), suggesting that the targeting of hPuf-A to the nucleolus not only depends on a long stretch of basic residues but also requires the presence of certain RNAs. RNA immunoprecipitation may help elucidate which RNA molecules are required for the distribution of hPuf-A in the nucleolus.

The amino-terminal DNA-binding domain of PARP-1 is important for the binding of PARP-1 to single-strand and double-strand breaks. The central automodification domain contains specific glutamate and lysine residues to serve as acceptors of ADP-ribose moieties that allow the enzyme to poly(ADP-ribose)ylation (22). Proteins containing macrodomain (26–28), pADPr-binding zinc finger (PBZ; ref. 29), or 8-amino acid motif (30) have been shown to associate with the pADPr moieties of PARP-1 in cells. The C-terminal catalytic domain sequentially transfers ADP-ribose subunits from NAD $^{+}$  to protein acceptors that associate with PARP-1. pADPr is structurally similar to RNA-like polymer with 2 ribose moieties and 2 phosphates in each structural unit of the polymer (22). It is plausible to propose that hPuf-A, a putative

RNA-binding protein, may preferentially bind pADPr-modified PARP-1 when hPuf-A leaves the nucleolus. Indeed, we observed an elevated level of hPuf-A-associated PARP-1 after UV or CPT treatment (Fig. 6B). If this were the scenario, hPuf-A should bind to the automodification domain of PARP-1. Nonetheless, hPuf-A does not contain macrodomain, PBZ, or 8-amino acid motif to associate with pADPr of automodification domain in PARP-1. Instead, hPuf-A interacted with the catalytic domain of PARP-1 to inhibit its pADPr activity (Fig. 6D). Preliminary data did not show a significant change in the levels of poly(ADP-ribose)ylation (Supplementary Fig. S7), suggesting that hPuf-A may not inhibit other members of the PARP family. Indeed, preliminary results did not show an association of hPuf-A with PARP-16 (data not shown). In addition, accumulated amounts of phosphorylated RPA2 and  $\gamma$ -H2AX on the chromatin highlight a possibility that DNA breaks are not sufficiently repaired in hPuf-A-depleted cells after CPT treatment, partly due to a decreased amount of PARP-1. Furthermore, although there is no consensus caspase cleavage motif in hPuf-A, it is likely that the stability of hPuf-A may be regulated by other proteolytic process that can generate a small peptide, RTLDKVLEV, presented as an mHAg.



**Figure 7.** hPuf-A attenuated PARP-1 cleavage by caspase-3. A, hPuf-A-depleted and -overexpressing cells were treated with CPT and UV light for 2 hours, respectively. Total cell extracts were collected and immunoblotted with the indicated antibodies. B, hPuf-A knockdown cells were treated with CPT (5  $\mu\text{mol/L}$ ) or CPT plus Z-DEVD-FMK (4  $\mu\text{mol/L}$ ) for 4 hours. Cell extracts were prepared to detect cleaved PARP-1. C, hPuf-A knockdown cells were treated with CPT (5  $\mu\text{mol/L}$ ) for 4 hours and chromatin-bound fractions were isolated for immunoblotting analysis by using the indicated antibodies.



## Disclosure of Potential Conflicts of Interest

No potential conflicts of interest were disclosed.

## Acknowledgments

We are grateful to Dr. Geen-Dong Chang for critical comments on this article and the staffs of TC5 Bio-Image Tools, College of Life Science, National Taiwan University, for assistance with confocal laser scanning microscopy.

## References

- Wickens M, Bernstein DS, Kimble J, Parker R. A PUF family portrait: 3'UTR regulation as a way of life. *Trends Genet* 2002;18:150-7.
- Wang X, McLachlan J, Zamore PD, Hall TM. Modular recognition of RNA by a human Pumilio-homology domain. *Cell* 2002;110:501-12.
- Lu G, Dolgner SJ, Hall TM. Understanding and engineering RNA sequence specificity of PUF proteins. *Curr Opin Struct Biol* 2009;19:110-5.
- Kuo MW, Wang SH, Chang JC, Chang CH, Huang LJ, Lin HH, et al. A novel puf-A gene predicted from evolutionary analysis is involved in the development of eyes and primordial germ-cells. *PLoS One* 2009;4:e4980.
- Kim MY, Zhang T, Kraus WL. Poly(ADP-ribosyl)ation by PARP-1: "PAR-laying" NAD<sup>+</sup> into a nuclear signal. *Genes Dev* 2005;19:1951-67.
- Hakmé A, Wong HK, Dantzer F, Schreiber V. The expanding field of poly(ADP-ribosyl)ation reactions. *EMBO Rep* 2009;9:1094-100.
- Rancourt A, Satoh MS. Delocalization of nucleolar poly(ADP-ribose) polymerase-1 to the nucleoplasm and its novel link to cellular sensitivity to DNA damage. *DNA Repair* 2009;8:286-97.
- Andrabi SA, Kim NS, Yu SW, Wang H, Koh DW, Sasaki M, et al. Poly (ADP-ribose) polymer is a death signal. *Proc Natl Acad Sci USA* 2006;103:18308-13.

## Grant Support

This work was supported by grants from National Science Council (NSC 99-2311-B-002-005) and National Taiwan University (99R80837) to M-S. Chang.

The costs of publication of this article were defrayed in part by the payment of page charges. This article must therefore be hereby marked *advertisement* in accordance with 18 U.S.C. Section 1734 solely to indicate this fact.

Received May 27, 2010; revised November 15, 2010; accepted December 2, 2010; published OnlineFirst January 25, 2011.



9. Yu SW, Wang H, Poitras MF, Coombs C, Bowers WJ, Federoff HJ, et al. Mediation of poly(ADP-ribose) polymerase-1-dependent cell death by apoptosis-inducing factor. *Science* 2002;297:259–63.
10. Yu SW, Andrabi SA, Wang H, Kim NS, Poirier GG, Dawson TM, et al. Apoptosis-inducing factor mediates poly(ADP-ribose) (PAR) polymer-induced cell death. *PNAS* 2006;103:18314–9.
11. Soldani S, Scovassi AI. Poly(ADP-ribose) polymerase-1 cleavage during apoptosis: an update. *Apoptosis* 2002;7:321–8.
12. Kim JW, Won J, Sohn S, Joe CO. DNA-binding activity of the N-terminal cleavage product of poly(ADP-ribose) polymerase is required for UV mediated apoptosis. *J Cell Sci* 2000;113:955–61.
13. Yung TM, Satoh MS. Functional competition between poly(ADP-ribose) polymerase and its 24-kDa apoptotic fragment in DNA repair and transcription. *J Biol Chem* 2001;276:11279–86.
14. Kim JW, Kim K, Kang K, Joe CO. Inhibition of homodimerization of poly(ADP-ribose) polymerase by its C-terminal cleavage products produced during apoptosis. *J Biol Chem* 2000;275:8121–5.
15. Brickner AG, Warren EH, Caldwell JA, Akatsuka Y, Golovina TN. The immunogenicity of a new human minor histocompatibility antigen results from differential antigen processing. *J Exp Med* 2001;193:195–205.
16. Méndez J, Stillman B. Chromatin association of human origin recognition complex, cdc6, and minichromosome maintenance proteins during the cell cycle: assembly of prereplication complexes in late mitosis. *Mol Cell Biol* 2000;20:8602–12.
17. Chu PC, Yang YC, Lu YT, Chen HT, Yu LC, Chang MS. Silencing of p29 affects DNA damage responses with UV irradiation. *Cancer Res* 2006;66:8484–91.
18. Gu W, Deng Y, Zenklusen D, Singer RH. A new yeast PUF family protein, Puf6p, represses ASH1 mRNA translation and is required for its localization. *Genes Dev* 2004;18:1452–65.
19. Deng Y, Singer RH, Gu W. Translation of ASH1 mRNA is repressed by Puf6p-Fun12p/elf5B interaction and released by CK2 phosphorylation. *Genes Dev* 2008;22:1037–50.
20. Shen Z, Paquin N, Forget A, Chartrand P. Nuclear shuttling of She2p couples ASH1 mRNA localization to its translational repression by recruiting Loc1p and Puf6p. *Mol Biol Cell* 2009;20:2265–75.
21. Andersen JS, Lam YW, Leung AKL, Ong SE, Lyon CE, Lamond AI, et al. Nucleolar proteome dynamics. *Nature* 2005;433:77–83.
22. Rouleau M, Patel A, Hendzel MJ, Kaufmann SH, Poirier GG. PARP inhibition: PARP1 and beyond. *Nat Rev Cancer* 2010;10:293–301.
23. Boisvert FM, van Koningsbruggen S, Navascués J, Lamond AI. The multifunctional nucleolus. *Nat Rev Mol Cell Biol* 2007;8:574–85.
24. Lam YW, Lamond AI, Mann M, Andersen JS. Analysis of nucleolar protein dynamics reveals the nuclear degradation of ribosomal proteins. *Curr Biol* 2007;17:749–60.
25. Emmott E, Hiscox JA. Nucleolar targeting: the hub of the matter. *EMBO Rep* 2009;10:231–238.
26. Ahel D, Horejsi Z, Weichens N, Polo SE, Garcia-Wilson E, Ahel I, et al. Poly(ADP-ribose)-dependent regulation of DNA repair by the chromatin remodeling enzyme ALC1. *Science* 2009;325:1240–3.
27. Gottschalk AJ, Timinszky G, Kong SE, Jin J, Cai Y, Swanson SK, et al. Poly(ADP-ribosyl)ation directs recruitment and activation of an ATP-dependent chromatin remodeler. *Proc Natl Acad Sci U S A* 2009;106:13770–4.
28. Timinszky G, Till S, Hassa PO, Hothorn M, Kustatscher G, Nijmeijer B, et al. A macrodomain-containing histone rearranges chromatin upon sensing PARP1 activation. *Nat Struct Mol Biol* 2009;16:923–9.
29. Ahel I, Ahel D, Matsusaka T, Clark AJ, Pines J, Boulton SJ, et al. Poly(ADP-ribose)-binding zinc finger motifs in DNA repair/checkpoint proteins. *Nature* 2008;451:81–5.
30. Gangne JP, Isabelle M, Lo KS, Boruassa S, Hendzel MJ, Dawson VL, et al. Proteome-wide identification of poly(ADP-ribose)-associated protein complexes. *Nucleic Acids Res* 2008;36:6959–76.

# Cancer Research

The Journal of Cancer Research (1916–1930) | The American Journal of Cancer (1931–1940)

## hPuf-A/KIAA0020 Modulates PARP-1 Cleavage upon Genotoxic Stress

Hao-Yen Chang, Chi-Chen Fan, Po-Chen Chu, et al.

*Cancer Res* 2011;71:1126-1134. Published OnlineFirst February 1, 2011.

<b>Updated version</b>	Access the most recent version of this article at: doi: <a href="https://doi.org/10.1158/0008-5472.CAN-10-1831">10.1158/0008-5472.CAN-10-1831</a>
<b>Supplementary Material</b>	Access the most recent supplemental material at: <a href="http://cancerres.aacrjournals.org/content/suppl/2011/01/25/0008-5472.CAN-10-1831.DC1">http://cancerres.aacrjournals.org/content/suppl/2011/01/25/0008-5472.CAN-10-1831.DC1</a>

<b>Cited articles</b>	This article cites 30 articles, 15 of which you can access for free at: <a href="http://cancerres.aacrjournals.org/content/71/3/1126.full#ref-list-1">http://cancerres.aacrjournals.org/content/71/3/1126.full#ref-list-1</a>
<b>Citing articles</b>	This article has been cited by 4 HighWire-hosted articles. Access the articles at: <a href="http://cancerres.aacrjournals.org/content/71/3/1126.full#related-urls">http://cancerres.aacrjournals.org/content/71/3/1126.full#related-urls</a>

<b>E-mail alerts</b>	<a href="#">Sign up to receive free email-alerts</a> related to this article or journal.
<b>Reprints and Subscriptions</b>	To order reprints of this article or to subscribe to the journal, contact the AACR Publications Department at <a href="mailto:pubs@aacr.org">pubs@aacr.org</a> .
<b>Permissions</b>	To request permission to re-use all or part of this article, use this link <a href="http://cancerres.aacrjournals.org/content/71/3/1126">http://cancerres.aacrjournals.org/content/71/3/1126</a> . Click on "Request Permissions" which will take you to the Copyright Clearance Center's (CCC) Rightslink site.